Chinese Chemical Letters 35 (2024) 108661

Contents lists available at ScienceDirect

Chinese Chemical Letters

journal homepage: www.elsevier.com/locate/cclet

Sensitizing photoactive metal–organic frameworks *via* chromophore for significantly boosting photosynthesis

Lihua Ma[a], Song Guo[b,*], Zhi-Ming Zhang[b], Jin-Zhong Wang[a,*], Tong-Bu Lu[b], Xian-Shun Zeng[a,b,*]

[a] School of Materials Science and Engineering, Harbin Institute of Technology, Harbin 150001, China
[b] Institute for New Energy Materials and Low Carbon Technologies, School of Material Science & Engineering, Tianjin University of Technology, Tianjin 300384, China

ARTICLE INFO

Article history:
Received 9 February 2023
Revised 29 April 2023
Accepted 7 June 2023
Available online 11 June 2023

Keywords:
Metal–organic framework
Photocatalysis
Excited state
Strong visible absorption
Iridium complex

ABSTRACT

Photosensitization related to energy/electron transfer process is of great importance to natural photosynthesis. Herein, we proposed a promising strategy to improve the sensitizing ability of the typical photoactive MOFs (**UiO-Ir**) by engineering its metal coordination center with NBI (1,8-naphthalenebenzimidizole) chromophore. The resulting MOFs (**UiO-Ir-NBI**) exhibited a strong sensitizing ability for significantly boosting photosynthesis. Impressively, the catalytic yield of 2-chloroethyl ethyl sulfoxide with **UiO-Ir-NBI** can reach 99%, over 6 times higher than that with **UiO-Ir** (16.4%). Moreover, **UiO-Ir-NBI** exhibited an excellent catalytic stability and a broad substrate tolerance, highlighting its great application prospect. Systematic investigations revealed that the strong visible light absorption, long excited state lifetime and efficient electron-hole separation of **UiO-Ir-NBI** greatly contributed to harvesting visible light and facilitating interface electron/energy transfer for efficient solar energy utilization. This work provides a new horizon to boost photosythesis of MOFs by engineering their metal sensitizing centers at a molecular level.

Sunlight has been regarded as the most promising renewable energy source to meet humanity's future energy demand due to its advantages in clean and inexhaustible [1–3]. Photosynthesis in plant represent the most successful example for solar energy utilization, which can massively transform the low energy density of sunlight into the available carbohydrate compounds [4]. In view of this, chemists have long been devoted to developing photocatalysts to mimic natural process. Thanks to their similar structural features with chlorophyll and the ease of their structure/property tuning, transition metal complexes have been widely used as molecular antenna for solar energy conversion [5–8]. For example, the typical $[Ru(bpy)_3]^{2+}$ (bpy = 2,2′-bipyridine) or $[Ir(ppy)_2(bpy)]^+$ (ppy = 2-phenylpyridine) derivatives have been applied to a range of energy-storing reactions for the past half a century [9–14]. The work mechanism of these complexes was usually as follows: upon light irridiation, charge transfer from metal to ligand was triggered to afford the singlet state (^{1}MLCT) and then it converted into the triplet excited state (^{3}MLCT) *via* intersystem crossing (ISC), which can further initial the intermolecular electron/energy tranfer process [6]. This process reveal that both visible light absorbing ability and excited state lifetime of complexes have a significant influence on their catalytic performance. Several attempts have made to couple the typcial Ru/Ir complexes with organic chromohores to enhance visible absorption and extend excited state lifetime, which have been confirmed as an efficient stratgy to improve the photosynthetic efficiency [15–18]. Nevertheless, these metal complexes are homogeneous in solution, which have some intrinsic drawbacks in humble catalytic stability, poor recyclable and excited state self-quenching. As a result, it's highly desirable but remains a great challenge to pursue the further development of strong sensitzing heterogeneous photocatalysts for efficient and sustainable photosynthesis.

As a class of crystalline porous materials, metal-organic frameworks (MOFs) have provided an ideal molecular platform to meet different application scenarios by precisely regulating their organic ligands, inorganic second building units (SBUs) or channels [19–28]. Of particular interest is to develop MOF photocatalysts for solar energy conversion associated with a series of processes of light absorption, interface- and intra-framework electron/energy transfer [29–34]. However, the traditional MOFs with

* Corresponding authors.
E-mail addresses: guosong@email.tjut.edu.cn (S. Guo), jinzhong.wang@hit.edu.cn (J.-Z. Wang), Xshzeng@tjut.edu.cn (X.-S. Zeng).

https://doi.org/10.1016/j.cclet.2023.108661
1001-8417/

terephthalic acid ligands or its derivatives such as UiO-66 and UiO-67 can just harvest ultraviolet (UV) light, which severely limited their solar energy utilization [34]. In order to overcome this limitation, attempts have been made to replace the traditional ligands with polypyridinal Ru/Ir complexes in MOFs for enhancing their visible light absorbing ability [30,35–40]. In this field, Lin *et al.* doped $[Ir(ppy)_2(dcbpy)]Cl$ and $[Ru(bpy)_2(dcbpy)]Cl_2$ into UiO-MOFs for visible light induced heterogeneous photosynthesis [41]. Chen *et al.* co-doped $[Ru(dcbpy)(bpy)_2]^{2+}$ (dcbpy = 2,2′-bipyridyl-5,5′-dicarboxylic acid) photosensitizer and $Pt(dcbpy)Cl_2$ catalyst into UiO-MOFs for photochemical conversion of H_2O to H_2 [42]. Kong *et al.* explored a $Ru(Phen)_3{}^{2+}$-based (Phen = phenanthroline) Eu-MOF for photocatalytic CO_2 reduction [43]. In addition, sorts of single sites and nano-clusters catalysts were introduced into the Ru/Ir complexes sensitized MOFs *via* ligand or channel modification for facilitating intra-framework electron transfer [44–48]. Despite this great progress on co-doping and engineering catalytic centers, the study on sensitizing center is still rare for photoactive MOFs [49–54]. The performance for MOF photocatalysts with the typical Ru/Ir complexes was limited by their poor visible light harvesting ability and relative short excited lifetime. Subsequently, we hypothesized that the catalytic performance of these MOFs is promising to be improved significantly by engineering the metal sensitizing center to enhance the visible absorption and impetus interface electron transfer.

Bearing these aspects in mind, we proposed a strategy to significantly improve the sensitizing ability of the typical photoactive UiO-MOFs (**UiO-Ir**) by engineering the Ir coordination center with NBI (1,8-naphthalenebenzimidizole) chromophore (**UiO-Ir-NBI**). The coordination environment of Ir center in UiO67-Ir-ppy was regulated by replacing ppy ligand with NBI, resulting in the transformation of excited state distribution from ^{3}MLCT excited state to ^{3}IL state (IL = intraligand). Remarkably, the conversion rate for the detoxification of a sulfur mustard simulant can reach 99% with **UiO-Ir-NBI** as photocatalyst, over 6 times higher than that with the typical **UiO-Ir** (16.4%). Systematic investigations reveal that the visible light absorption, excited state lifetime and electron-hole separation of **UiO-Ir** were significantly improved *via* NBI sensitization, which contributed to efficiently harvesting visible light and facilitating interface electron/energy transfer for boosting photosynthesis. This work opens up a new avenue to significantly efficient boost photosythesis by engineering their sensitizing centers with chromophores.

Upon excitation, ^{3}MLCT state was populated in the traditional Ru-/Ir-based photoactive MOFs, resulting in weak visible absorption and short excited state lifetime, which was harmful to the interface electron/energy transfer and sunlight utilization. To tackle these issues, we tried to improve photosensitization of the MOFs by engineering their metal sensitizing center with organic chromophores. The design concept of this strategy is to enhance visible harvesting ability and prolong the excited state lifetime of MOFs *via* altering their light absorbing channel from ^{1}MLCT to π-π^* transition and switching their triplet state distribution from ^{3}MLCT state to ^{3}IL stae for boosting photosynthesis (Fig. 1a). The excited state distribution of photosensitizing units in **UiO-Ir** and **UiO-Ir-NBI** can be visualized by density function theory (DFT) calculation. As shown in Fig. 1, the spin density surface of **L-1** was distributed on the Ir center, ppy and 2,2′-bipyridine-5,5′-dicarboxylic acid, representing the typical MLCT excited state of cyclometalated Ir(III) complexes. After chromophore sensitization, the spin density surfaces distributed on NBI chromophore, Ir center and 2,2′-bipyridine-5,5′-dicarboxylic acid in **L-2**, assigned to the mixed state of ^{3}MLCT /^{3}IL excited state.

Under the guidance of design principle, NBI chromophore was used to sensitize the Ir sensitizing center of the typical UiO-Ir to afford **UiO-Ir-NBI** *via* bottom-up synthetic approach. As shown in

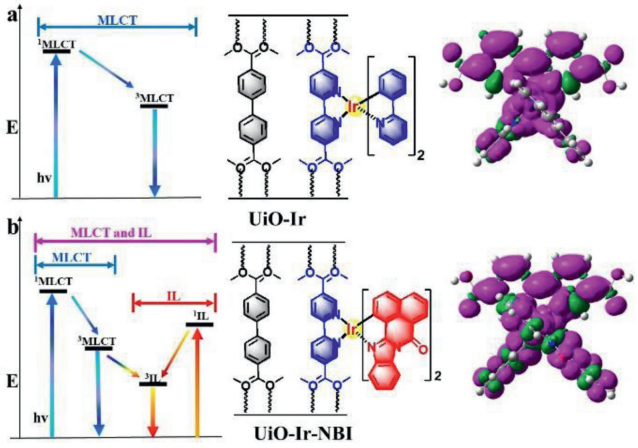

Fig. 1. (a) Schematic show of the energy level of MOFs with ^{3}MLCT excited state, the structure of **UiO-Ir** and electron spin density of **L-1**. (b) Schematic show of the energy level of MOFs with ^{3}MLCT/^{3}IL excited state, the structure of **UiO-Ir-NBI** and electron spin density of **L-2**.

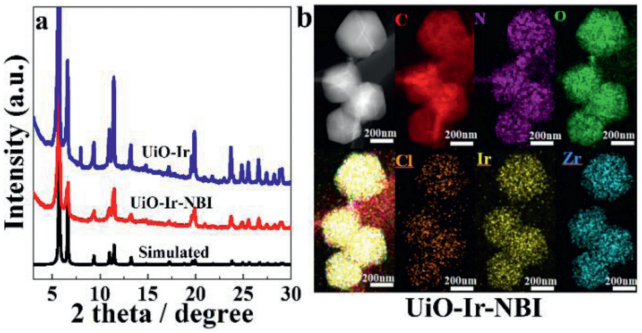

Fig. 2. (a) PXRD patterns of **UiO-Ir** and **UiO-Ir-NBI**. (b) High angle annular dark field scanning transmission electron microscopy and elemental mapping images for **UiO-Ir-NBI**.

Scheme S1 (Supporting information), the synthetic process of **L-2** was similar to that of the typical **L-1**. Iridium dimer (**6**) was prepared by coordinating NBI chomophore with $IrCl_3{\cdot}3H_2O$, which can further react with 5,5′-dimethoxycarbonyl-2,2′-bipyridine to generate complex **7**. Subsequently, **L-2** can be achieved *via* hydrolysis of complex **7**. According to the typical synthesis route of UiO-MOFs, the mixture of **L-2**, $ZrCl_4$ and 4,4'-biphenyldicarboxylic acid (**8**) was dissloved in *N*,*N*-dimethylformamide (DMF) and heated at 100 °C for 24 h to afford the photosensitizing MOF **UiO-Ir-NBI**. The structures of organic intermediates and ligands were characterized by ^{1}H nuclear magnetic resonance (NMR) and high resolution mass spectrometer (HRMS) (Figs. S1-S9 in Supporting information). Both **UiO-Ir-NBI** and **UiO-Ir** presented a similar powder X-ray diffraction (PXRD), which well matched with the simulated crystal data of UiO-67 (Fig. 2a). This result manifested that the introdution of **L-2** did not significantly disturb the structure and crystallinity of UiO-67. A shape of close to octahedron was observed for **UiO-Ir-NBI** by scanning electron microscope (SEM) (Fig. S10 in Supporting information). Besides, elemental mapping images showed the adequate distribution of Zr, Ir, Cl, C, N and O elements in **UiO-Ir-NBI**, supporting that **L-2** was successfully introduced into UiO-67 (Fig. 2b). X-ray photoelectron spectroscopy (XPS) was carried out on **UiO-Ir-NBI** to determine the valence state of Ir in MOFs. As shown in Fig. S11 (Supporting information), two peaks at around 62.3 and 65.3 eV were observed in Ir 4f region, which can be attributed to Ir $4f_{7/2}$ and $4f_{5/2}$ of Ir^{3+}. As a result, the valence state of Ir in MOFs was estimated as +3, well matched with that in **L-2**. Furthermore, according to the results of inductively coupled plasma-mass spec-

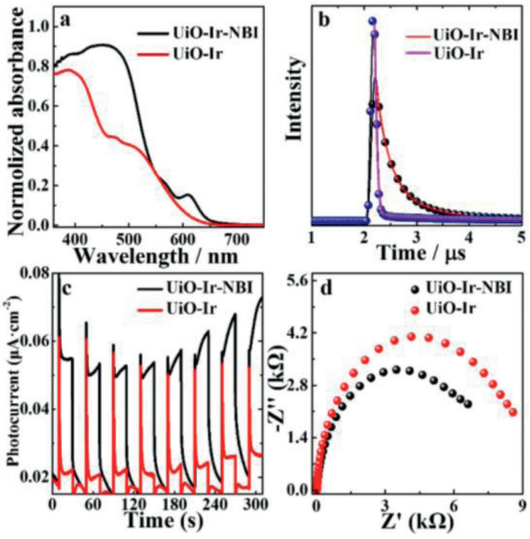

Fig. 3. (a) UV–Vis absorption spectra of **UiO-Ir-NBI** and **UiO-Ir**. (b) Photoluminescence lifetime of **UiO-Ir-NBI** and **UiO-Ir**. (c) Photocurrent response and (d) Nyquist of **UiO-Ir-NBI** and **UiO-Ir**.

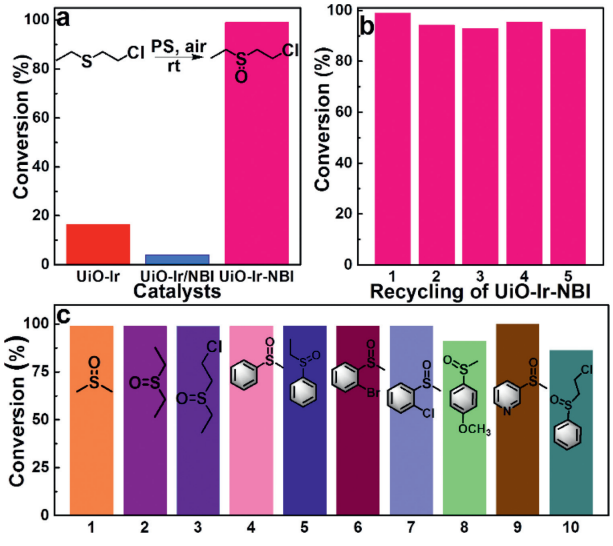

Fig. 4. (a) Catalytic activities of **UiO-Ir-NBI**, **UiO-Ir** and **UiO-Ir**/NBI for photo-oxidation of sulfide. (b) Recycling experiments with **UiO-Ir-NBI**. (c) The catalytic performance of **UiO-Ir-NBI** for different substrates.

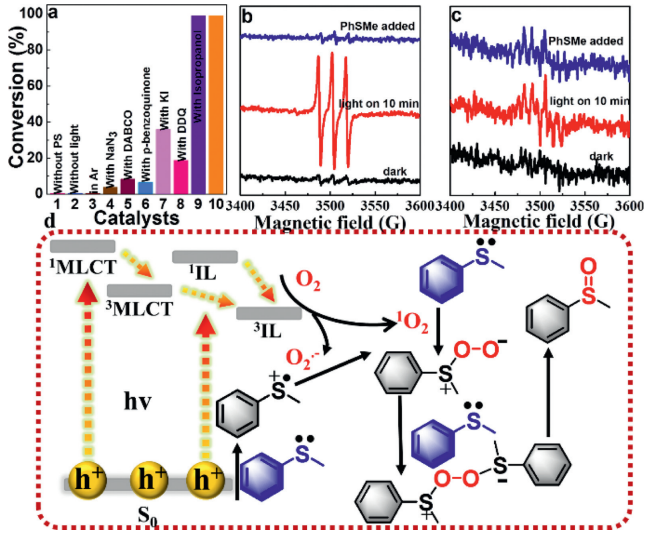

Fig. 5. (a) Control experiments of **UiO-Ir-NBI** for photocatalytic sulfoxidation reaction. (b, c) ESR spectra of **UiO-Ir-NBI** in the presence of 4-oxo-TMP and DMPO in CH_3OH. The black line represents under dark, the red line represents under light and the blue line represents with thioanisole under light. (d) The proposed mechanism for photo-oxidation of thioanisole.

trometry (ICP-MS) test, the Ir content in **UiO-Ir-NBI** and **UiO-Ir** was detemined to be 158 μmol/g and 157 μmol/g, respectively, excluding the potential influence of Ir loading amount in different MOFs on their photosynthetic performance.

The photoelectrochemical properties of **UiO-Ir-NBI** and **UiO-Ir** were sysmetically investigated by steady, transient and photoelectrochemical spectra (Fig. 3). As shown in Fig. 3a, **UiO-Ir-NBI** presented a strong visible light absorption between 400 nm and 650 nm, significantly stronger than that of traditional **UiO-Ir**, indicating a more efficient solar energy utilization for **UiO-Ir-NBI**. The transient absorption of **L-2** exhibited a bleaching between 420 nm and 480 nm, which could be attributed that is triplet state was localized on the NBI ligand (Fig. S12 in Supporting information). This result well matched with spin density distribution of **L-2** (Fig. 1). In addition, the excited state lifetime of UiO-MOFs extended from 0.7 μs for **UiO-Ir** to 1.2 μs for **UiO-Ir-NBI**, which contributed to promoting its interface electron/energy transfer (Fig. 3b). As compared with **UiO-Ir**, **UiO-Ir-NBI** exhibited a strong and sharp phosphorescence, indicating its weak triplet-triplet annihilation and efficient triplet population, which contributed to facilitating interface electron transfer (Fig. S13 in Supporting information). Photocurrent measurements reveal that **UiO-Ir-NBI** exhibits a stronger photocurrent response than **UiO-Ir**, confirming a more efficient photogenerated electron-hole separation for the former (Fig. 3c). This viewpoint was also supported by electro-chemical impedance spectroscopy (EIS), where **UiO-Ir-NBI** showed a smaller radius and a lower resistance for charge transfer than **UiO-Ir** (Fig. 3d). Subsequently, the advantages of **UiO-Ir-NBI** in strong visible light absorbing ability, long excited state lifetime and efficient electron-hole seperation, higlighting its great potential on energy- and eletron transfer photoreaction.

In view of the superior photoelectrochemical properties of **UiO-Ir-NBI**, it was used for photo-oxidation of sulfide to exam its sensitzing ability (Fig. 4 and Tables S1-S3 in Supporting information). 2-Chloroethyl ethyl sulfide is a chemical warfare agent simulant of mustard gas, which can be oxidized into nontoxic 2-chloroethyl ethyl sulfoxide by using light as driven force and O_2 as green oxidant. Notably, the 2-chloroethyl ethyl sulfoxide yield with **UiO-Ir-NBI** was as high as 99% within 30 min, over 6 and 24 times higher than that with **UiO-Ir** and the mixture of **UiO-Ir**/NBI, respectively. This result indicates that it is necessary to directly coordinate NBI chromophore to Ir sensitizing center for efficient synergism between NBI and Ir center. Besides, **UiO-Ir-NBI** exhibited an outstanding catalytic stability, which can be recycled for 5 times without abvious structrue change and activity loss (Figs. S14 and S15 in Supporting information). Furthermore, **UiO-Ir-NBI** can photo-oxidize various aromatic sulfides and alkyl sulfides into the corresponding sulfoxides with over 90% yield, indicating an excellent substrate tollerance (Table S3).

In order to unveil the distinguished catalytic performance of **UiO-Ir-NBI**, the catalytic mechanism was comprehensively investigated by a series of control experiments and electron spin-resonance (ESR) tests (Fig. 5 and Table S4 in Supporting information). Almost no product was detected without MOF PS, light or O_2, indicating that all above factors are essential for efficient photo-oxidation. Both NaN_3 and 1,4-diazabicyclooctane (DABCO) were the typical $^1O_2$ trapping agent. After adding NaN_3 or DABCO, the yield of methyl phenyl sulfoxide significantly decreased to 3.8% or 8.3%.

In the presence of p-benzoquinone as a $^{\bullet}O_2^-$ scavenger, the catalytic yield also decreased to 6.5%. These results preliminarily confirmed that both $^1O_2$ and $^{\bullet}O_2^-$ were the important oxidant for efficient photosynthesis. In addition, the catalytic yield was detemined to be 35.9% with KI as a hole scavenger and 18.7% with DDQ as an electron scavenger, indicating that the electron transfer pathway played an important role in catalytic process. A yield of 99.0% was obtained in the prescence of isopropanol as an $^{\bullet}OH$ radical scavenger, excluding the possibility that $^{\bullet}OH$ participated in catalytic reaction. Furthermore, ESR measurements were performed to further discern the reactive oxygen species (ROS) [55]. 4-oxo-TMP and 5,5-dimethyl-1-pyrroline *N*-oxide (DMPO) were employed as $^1O_2$ and $^{\bullet}O_2^-$ trapping agents, respectively. Upon irridiation, the strong triple peaks were emerged in the presence of 4-oxo-TMP, which was the typical characteristic signal of adduct of $^1O_2$–4-oxo-TMP (Fig. 5b). This characteristic signal significantly decreased after adding methyl phenyl sulfoxide. Meanwhile, the characteristic signal of the $^{\bullet}O_2^-$TEMPO complex was also observed, which decreased after the addition of substrate (Fig. 5c). These results further supported that both $^1O_2$ and $^{\bullet}O_2^-$ was indeed a ROS for efficient photo-oxidation of sulfide.

Accordingly, the catalytic mechanism was proposed as follows (Fig. 5d): (1) Upon light excitation, **UiO-Ir-NBI** can efficient harvest visible light *via* dual absorbing channels of $S_o \rightarrow {}^1$MLCT and $S_o \rightarrow {}^1$IL to attain ^{1}MLCT/^{1}IL state. After a series of intramolecular photophysical processes, a long-lived ^{3}IL state was achieved for **UiO-Ir-NBI**, which contributed to interface electron/energy transfer. (2) ^{3}IL state of **UiO-Ir-NBI** can efficiently transfer energy/electron to O_2 to produce $^1O_2$ and $^{\bullet}O_2^-$, respectively. Besides, the HOMO of **UiO-Ir-NBI** can accept the electron from thioanisole to afford the reduced **UiO-Ir-NBI**, which can further deliver electron to O_2 to promote the generation of $^{\bullet}O_2^-$. (3) Both $^1O_2$ and $^{\bullet}O_2^-$can efficiently photo-oxidize sulfides into the sulfoxides product. As a result, as compared with the typical **UiO-Ir**, the long-lived ^{3}IL state and the new absorbing channel from S_o to ^{1}IL of **UiO-Ir-NBI** can facilitate interface electron/energy transfer and solar energy utilization, which greatly contributed to boosting photosynthesis.

We have explored a strategy to improve the sensitzing ability of MOFs *via* engineering their metal sensitizing center for dramatically boosting photosynthesis. A novel strong sensitizing MOF **UiO-Ir-NBI** was prepared by replacing ppy ligand of the typical UiO67-Ir with NBI ligand, which established a strong visible absorbing channel from S_o to ^{1}IL and a long-lived ^{3}IL excited state. Impressively, the catalytic yield of 2-chloroethyl ethyl sulfoxide with **UiO-Ir-NBI** photocatalyst can reach to 99%, over 6 times higher than that with the typical **UiO-Ir** (16.4%). In addition, **UiO-Ir-NBI** exhibited an excellent catalytic stability and a broad substrate tolerance, highlighting its great potential for practical application. Systematical investigations revealed that the superior properties of **UiO-Ir-NBI** in strong visible light absorption, long excited state lifetime and efficient electron-hole separation contributed to efficiently harvesting visible light and facilitating interface electron/energy transfer for boosting photosynthesis. This work not only develops a strong sensitizing MOF photocatalyst, but also provides a new horizon to significantly boost photosythesis by engineering their metal sensitizing centers with chromophores.

Declaration of competing interest

The authors declare that they have no known competing financial interests or personal relationships that could have appeared to influence the work reported in this paper.

Acknowledgments

This work was supported by National Key R&D Program of China (No. 2019YFA0705201), National Natural Science Foundation of China (No. 22171209).

Supplementary materials

Supplementary material associated with this article can be found, in the online version, at doi:10.1016/j.cclet.2023.108661.

References

[1] Y.J. Yuan, Z.T. Y.u, D.Q. Chen, et al., Chem. Soc. Rev. 33 (2017) 603–631.
[2] Y. Tachibana, L. Vayssieres, J.R. Durrant, Nat. Photonics 6 (2012) 511–518.
[3] X.B. Li, C.H. Tung, L.Z. Wu, Nat. Rev. Chem. 2 (2018) 160–173.
[4] T. Mirkovic, E.E. Ostroumov, J.M. Anna, et al., Chem. Rev. 117 (2017) 249–293.
[5] D.N. Tritton, F.K. Tang, G.B. Bodedla, et al., Coord. Chem. Rev. 459 (2022) 214390.
[6] C.K. Prier, D.A. Rankic, D.W. MacMillan, Chem. Rev. 113 (2013) 5322–5363.
[7] B.G. Cai, J. Xuan, W.J. Xiao, Sci. Bull. 64 (2019) 337–350.
[8] A.K. Pal, G.S. Hanan, Chem. Soc. Rev. 43 (2014) 6184–6197.
[9] J. Zhao, W. Wu, J. Sun, et al., Chem. Soc. Rev. 42 (2013) 5323–5351.
[10] J. Zhao, S. Ji, W. Wu, et al., RSC Adv. 2 (2012) 1712–1728.
[11] S.Y. Takizawa, R. Aboshi, S. Murata, Photochem. Photobiol. Sci. 10 (2011) 895–903.
[12] J.I. Goldsmith, W.R. Hudson, M.S. Lowry, et al., J. Am. Chem. Soc. 127 (2005) 7502–7510.
[13] J. Jiang, B.D. Sherman, Y. Zhao, et al., ACS Appl. Mater. Interfaces 9 (2017) 19529–19534.
[14] L.Y. Zhang, S.Y. Yin, M. Pan, et al., J. Mater. Chem. A 5 (2017) 9807–9814.
[15] P. Wang, S. Guo, H.J. Wang, et al., Nat. Commun. 10 (2019) 3155.
[16] S. Guo, K.K. C.hen, R. Dong, et al., ACS Catal. 8 (2018) 8659–8670.
[17] L. Qin, R. Wang, X. Xin, et al., Appl. Catal. B 312 (2022) 121386.
[18] X. Zhao, Y. Hou, L. Liu, et al., Energy Fuels 35 (2021) 18942–18956.
[19] Y. Bai, Y. Dou, L.H. Xie, et al., Chem. Soc. Rev. 45 (2016) 2327–2367.
[20] A. Dhakshinamoorthy, Z. Li, H. Garcia, Chem. Soc. Rev. 47 (2018) 8134–8172.
[21] Q. Yang, Q. Xu, H.L. Jiang, Chem. Soc. Rev. 46 (2017) 4774–4808.
[22] B. Li, M. Chrzanowski, Y. Zhang, et al., Coord. Chem. Rev. 307 (2016) 106–129.
[23] X. Zhang, S. Tong, D. Huang, et al., Coord. Chem. Rev. 448 (2021) 214177.
[24] Z. Chen, S.L. H.anna, L.R. R.edfern, et al., Coord. Chem. Rev. 386 (2019) 32–49.
[25] V. Pascanu, G.G. Miera, A.K. Inge, et al., J. Am. Chem. Soc. 141 (2019) 7223–7234.
[26] K. Wang, Y. Li, L.H. Xie, et al., Chem. Soc. Rev. 51 (2022) 6417–6441.
[27] C.D. W.u, M. Zhao, Adv. Mater. 29 (2017) 1605446.
[28] H. Zheng, Y. Hou, S. Li, et al., Chin. Chem. Lett. 33 (2022) 5013–5022.
[29] J.D. X.iao, H.L. Jiang, Acc. Chem. Res. 52 (2018) 356–366.
[30] Y.H. Luo, L.Z. Dong, J. Liu, et al., Coord. Chem. Rev. 390 (2019) 86–126.
[31] Z. Liang, C. Qu, D. Xia, et al., Angew. Chem., Int. Ed. 57 (2018) 9604–9633.
[32] L. Zeng, X. Guo, C. He, et al., ACS Catal. 6 (2016) 7935–7947.
[33] A. Dhakshinamoorthy, A.M. Asiri, H. Garcia, Angew. Chem. Int. Ed. 55 (2016) 5414–5445.
[34] Y. Li, H. Xu, S. Ouyang, et al., Phys. Chem. Chem. Phys. 18 (2016) 7563–7572.
[35] T.C. Z.huo, Y. Song, G.L. Z.huang, et al., J. Am. Chem. Soc. 143 (2021) 6114–6122.
[36] Y.Y. Z.hu, G. Lan, Y. Fan, et al., Angew. Chem. Int. Ed. 57 (2018) 14090–14094.
[37] S. Yang, B. Pattengale, S. Lee, et al., ACS Energy Lett. 3 (2018) 532–539.
[38] S. Guo, L.H. Kong, P. Wang, et al., Angew. Chem. Int. Ed. 61 (2022) e202206193.
[39] D. Kim, D.R. Whang, S.Y. Park, J. Am. Chem. Soc. 138 (2016) 8698–8701.
[40] M.E. Mahmoud, H. Audi, A. Assoud, J. Am. Chem. Soc. 141 (2019) 7115–7121.
[41] C. Wang, Z. Xie, K.E. deKrafft, et al., J. Am. Chem. Soc. 133 (2011) 13445–13454.
[42] C.C. Hou, T.T. Li, S. Cao, et al., J. Mater. Chem. A. 3 (2015) 10386–10394.
[43] Z.H. Yan, M.H. Du, J. Liu, et al., Nat. Commun. 9 (2018) 3353.
[44] C. Wang, K.E. deKrafft, W. Lin, J. Am. Chem. Soc. 134 (2012) 7211–7214.
[45] Z.M. Zhang, T. Zhang, C. Wang, et al., J. Am. Chem. Soc. 137 (2015) 3197–3200.
[46] P.M. Stanley, C. Thomas, E. Thyrhaug, et al., ACS Catal. 11 (2021) 871–882.
[47] J. Li, L. He, Q. Liu, et al., Nat. Commun. 13 (2022) 928.
[48] P.M. Stanley, J. Haimerl, C. Thomas, et al., Angew. Chem. Int. Ed. 60 (2021) 17854–17860.
[49] L. Jiao, Y.Y. Dong, X. Xin, L. Qin, H.J. Lv, Appl. Catal. B: Environ. 291 (2021) 120091.
[50] L. Jiao, Y.Y. Dong, X. Xin, R.J. Wang, H.J. Lv, J. Mater. Chem. A 9 (2021) 19725–19733.
[51] R.J. Wang, Y.Q. Feng, L. Jiao, et al., J. Mater. Chem. A 11 (2023) 5811–5818.
[52] H. Yu, X. Wu, Q.Q. Mu, et al., Chin. Chem. Lett. 32 (2021) 3833–3836.
[53] H.Y. Ma, Y. Liu, R. Xiong, J.H. Wei, Chin. Chem. Lett. 33 (2022) 1042–1046.
[54] Y.X. Du, Y.T. Zhou, M.Z. Zhu, Tungsten 5 (2023) 201–216.
[55] K.X. Teng, L.Y. Niu, N. Xie, et al., Nat. Commun. 13 (2022) 6179.